Near Infrared Absorption of Pure Carbon Dioxide up to 3100 bar and 500 K. I. Wavenumber Range 3200 cm^{-1} to 5600 cm^{-1}

M. Buback, J. Schweer, and H. Tups

Institut für Physikalische Chemie der Universität Göttingen

Z. Naturforsch. **41 a,** 505–511 (1986); received December 7, 1985

Near infrared absorption of pure CO_2 in the $\nu_1 + \nu_3$, $2\nu_2^0 + \nu_3$ Fermi diad region around 3650 cm^{-1} and in the $2\nu_1 + \nu_3$, $\nu_1 + 2\nu_2^0 + \nu_3$, $4\nu_2^0 + \nu_3$ Fermi triad region around 5000 cm^{-1} was measured at temperatures between 298 K and 500 K to a maximum pressure of 3100 bar. Density tuning of Fermi resonance is studied and compared with literature data on gaseous, liquid, and solid CO_2. Band maximum positions determined within an extended temperature and density range indicate appreciable rotational freedom up to about the critical density (0.45 $g \cdot cm^{-3}$) and repulsive interactions clearly coming into play above 0.9 $g \cdot cm^{-3}$. The vibrational intensity of the Fermi triad, up to about 1.0 $g \cdot cm^{-3}$ is found to be independent of temperature and pressure within ± 2.5%, wich enables (pure) CO_2 concentrations in a large region of states to be precisely and directly measured via quantitative high-pressure high-temperature near infrared spectroscopy.

1. Introduction

Vibrational high-pressure spectroscopy on supercritical fluids enables gaseous and liquid-like states to be connected by a sequence of spectra measured at arbitrary intermediate densities. For several simple molecules, such a water [1], ammonia [2], ethylene [3], and carbon monoxide [4], changes in bandshape, molar absorptivity, and band maximum position have been studied at independent variation of density and temperature. By far most of these investigations have been performed on stretching fundamentals. During recent years an increasing interest in near infrared (NIR) combination and overtone modes has developed since vibrational intensities of some of these bands turned out to be independent of density and temperature, which allows concentrations in fluid phase equilibria and chemical reactions to be directly and precisely measured via quantitative high-pressure high-temperature NIR spectroscopy [5].

With respect to these analytical applications, NIR investigation of fluid carbon dioxide seemed rewarding: CO_2 occurs in a wide variety of chemical reactions at elevated pressures and temperatures. Phase equilibria with CO_2 receive increasing interest with main emphasis on supercritical fluid extraction [6, 7]. The fundamental modes of solid, liquid, and gaseous CO_2, including fluid states, have been extensively studied by infrared and Raman techniques [8–11] with special interest on the occurrence of Fermi resonance between the ν_1 stretching fundamental and the $2\nu_2^0$ bending overtone around 1300 cm^{-1}. NIR spectra have been reported for the dilute gaseous and for the dense liquid state and for solid CO_2 up to 120 kbar [8, 9, 12–19]. The purpose of the present paper is to study the NIR absorption from 3200 cm^{-1} to 5600 cm^{-1} of pure fluid CO_2 in an extended pressure and temperature range up to 3100 bar and 500 K, respectively, and to discuss the density and temperature dependence of band positions and of vibrational intensities.

Reprint requests to Prof. Dr. M. Buback, Institut für Physikal. Chemie der Universität Göttingen, Tammannstraße 6, D-3400 Göttingen.

2. Experimental

The optical cell for operation to 600 K and 3500 bar is described elsewhere [20]. Optical path lengths between 0.11 mm and 1.22 mm have been used. The cell is heated electrically from outside. Temperatures are measured to better than ± 0.5 K with a sheathed thermocouple inside the sample fluid. Pressures are determined with Bourdon gauges within ± 3 bar even at 3000 bar.

Spectra were recorded on a Bruker IFS 85 Fourier transform interferometer. Molar integrated absorp-

0340-4811 / 86 / 0300-0505 $ 01.30/0. – Please order a reprint rather than making your own copy.

tivities B are calculated according to

$$B = \int \varepsilon(\bar{\nu}) \cdot \mathrm{d}\bar{\nu}. \quad (1)$$

The molar absorptivity $\varepsilon(\bar{\nu})$ is obtained from the experimental spectra:

$$\varepsilon(\bar{\nu}) = A(\bar{\nu})/(c\,l). \quad (2)$$

$A(\bar{\nu})$ is the decadic absorbance, c the actual density as obtained from published PVT-data [21, 22], and l the optical path length, which has to be corrected for experimental pressure and temperature [20].

The uncertainties of $\varepsilon(\bar{\nu})$ in band maxima are $\pm$ 2.5%. Due to problems in the precise position of the baseline for integration, the accuracy of B is $\pm$ 5%. The wavenumbers of the band maxima are accurate within $\pm$ 1 cm^{-1}.

3. Results

NIR absorption of CO_2 between 3200 cm^{-1} and 5600 cm^{-1} consists of two band systems centered around 3650 cm^{-1} and 5000 cm^{-1}, respectively. The lower wavenumber absorption, which is assigned to the $\nu_1 + \nu_3$, $2\nu_2^0 + \nu_3$ Fermi diad, is shown in Figure 1. Absorbance spectra at 450 K are plotted for densities varying from bottom to top in steps of 0.1 g · cm^{-3} between 0.1 g · cm^{-3}, corresponding to 77 bar, and 0.8 g · cm^{-3}, corresponding to 849 bar (the curves are shifted in the baseline). For both vibrations, P- and R-type contours at low densities gradually transform into fairly symmetric single bands at high density.

The 5000 cm^{-1} band system consists of three components being assigned to the $2\nu_1 + \nu_3$, $\nu_1 + 2\nu_2^0 + \nu_3$, $4\nu_2^0 + \nu_3$ Fermi triad. Figure 2 shows absorption spectra at 350 K and densities varied in steps of 0.1 g · cm^{-3} from 0.1 g · cm^{-3} (54 bar) up to 1.2 g · cm^{-3} (2300 bar), which is slightly above the liquid triple point density (1.18 g · cm^{-3} at 216.6 K). These spectra also demonstrate the transition from P- und R-type contour to single bands at the highest densities. Above 0.9 g · cm^{-3} additional weak bands or shoulders are clearly oberved. The components at 4808 cm^{-1} and 5123 cm^{-1} are assigned to hot-band transitions [8].

The band maximum positions, $\bar{\nu}$(max), and vibrational intensities B determined from the spectra taken in the extended fluid range are presented and discussed in the subsequent section.

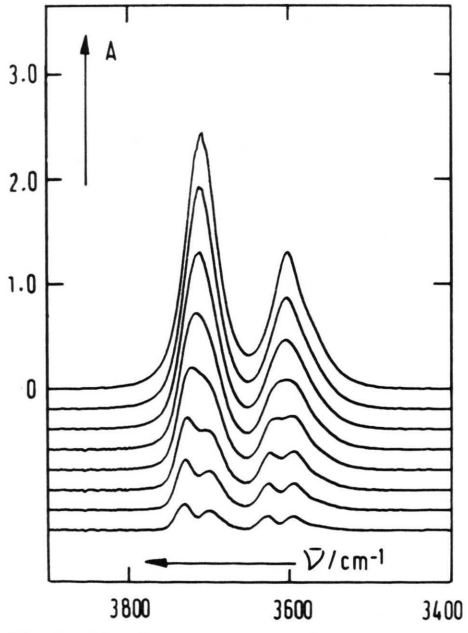

Fig. 1. Absorbance spectra of pure CO_2 at 450 K and densities varying – from bottom to top – in steps of 0.1 g · cm^{-3} between 0.1 g · cm^{-3} (77 bar) and 0.8 g · cm^{-3} (849 bar).

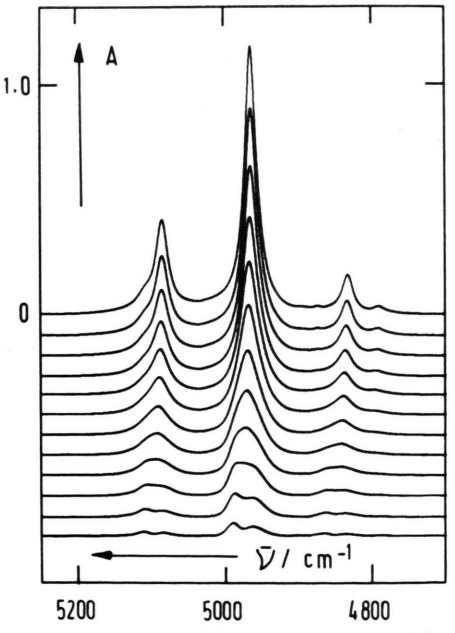

Fig. 2. Near infrared absorbance of pure CO_2 at 350 K and densities varying – from bottom to top – in steps of 0.1 g · cm^{-3} between 0.1 g · cm^{-3} (54 bar) and 1.2 g · cm^{-3} (2300 bar).

4. Discussion

The CO_2 molecule has $D_{\infty h}$ symmetry. The three fundamentals ν_1, ν_2, and ν_3 belong to irreducible representations Σ_g^+, Σ_u^+, and Π_u, respectively [8]. The vibrational states are fully characterized by quantum numbers v_1, v_2^l, v_3 with l being due to the degeneracy of ν_2. The gaseous infrared frequencies are $\bar{\nu}_2^g = 667.4\ cm^{-1}$ and $\bar{\nu}_3^g = 2349.1\ cm^{-1}$ [18]. The position of the ν_1 Raman active fundamental is less easily available because of Fermi resonance interaction with the bending first overtone component $2\nu_2^0$ giving rise to two bands of comparable intensity. This classical resonance situation has been extensively studied over the past 50 years [8–12, 17]. Only recently convincing evidence has accumulated on $\bar{\nu}_1^u > 2\bar{\nu}_2^{0,u}$, the unperturbed wavenumber of ν_1 being larger than the unperturbed bending overtone $2\nu_2^0$ in compressed gaseous, in liquid, and in solid CO_2 [11, 17]. The dilute gas, however, is close to the situation of perfect resonance ($\bar{\nu}_1^u = 2\bar{\nu}_2^{0,u}$) and several groups established $\bar{\nu}_1^u < 2\bar{\nu}_2^{0,u}$ for gaseous CO_2 at low pressure [11].

Fermi resonance coupling also occurs in all NIR combination modes containing ν_1 and/or $2\nu_2^0$, $4\nu_2^0$, $6\nu_2^0$ and so on. Thus the absorption around $3650\ cm^{-1}$ (Fig. 1) is due to the $\nu_1+\nu_3$, $2\nu_2^0+\nu_3$ Fermi diad, and the $5000\ cm^{-1}$ absorption is assigned to the $2\nu_1+\nu_3$, $\nu_1+2\nu_2^0+\nu_3$, $4\nu_2^0+\nu_3$ Fermi triad. (In the subsequent text $2\nu_2^0$ is replaced by $2\nu_2$ to simplify notations. It is understood that because of identical symmetry, ν_1 is in Fermi resonance with the $2\nu_2^0$ component.)

Close similarity of the resonance situation in the ν_1 fundamental and in the $\nu_1+\nu_3$ combination mode region is illustrated in Fig. 3 with ν_1, $2\nu_2$ Raman data and $\nu_1+\nu_3$, $2\nu_2+\nu_3$ NIR data of fluid and solid CO_2, respectively [10, 17]. The values of the wavenumber difference between ν_1 and $2\nu_2$ and between $\nu_1+\nu_3$ and $2\nu_2+\nu_3$ Fermi coupled species, $\Delta\bar{\nu}$, agree at fluid densities. (Individual band positions at moderate densities are determined from the arithmetic mean of P- and R-branches (Fig. 1) or from band centers at half peak height.) In solid CO_2 at high pressure, the absolute values of $\Delta\bar{\nu}$ determined from Raman ($\nu_1, 2\nu_2$) and NIR ($\nu_1+\nu_3$, $2\nu_2+\nu_3$) experiments [17] are slightly different. The density dependence of $\Delta\bar{\nu}$, however, is very similar for the two Fermi diads. The steep increase of $\Delta\bar{\nu}$ toward the highest densities demonstrates that pure stretching modes (ν_1) are shifted to higher and the pure ν_2 bending mode is shifted to lower wavenumbers as has been shown by Hanson and Jones [17].

Figure 4 further illustrates the similarity between the fundamental and the combination mode Fermi diads by relative integrated Raman scattering diad intensities $I(\nu_1)/I(2\nu_2)$ and relative NIR diad integrated molar absorptivities $B(\nu_1+\nu_3)/B(2\nu_2+\nu_3)$. (Because of Fermi resonance, the notations ν_1, $2\nu_2$, $\nu_1+\nu_3$, $2\nu_2+\nu_3$ are no correct assignments. The ratios of intensities (Fig. 4) are obtained by dividing the value for the higher wavenumber component through the corresponding lower wavenumber intensity.) The density dependence of both quantities is very similar at moderate and high fluid densities. In the solid state only Raman ($\nu_1, 2\nu_2$) data are available. The intensity ratio of the two components, as does $\Delta\bar{\nu}$ (Fig. 3), steeply increases with density.

The density tuning of the Fermi resonance as shown in Figs. 3 and 4 demonstrates the unperturbed wavenumbers of ν_1 being above $2\nu_2$ and of $\nu_1+\nu_3$ being above $2\nu_2+\nu_3$. Thus, throughout the density range of the present investigation, the higher wavenumber component within each of the two Fermi diads has the larger stretching mode character whereas the bending contribution dominates in the lower wavenumber component of both pairs.

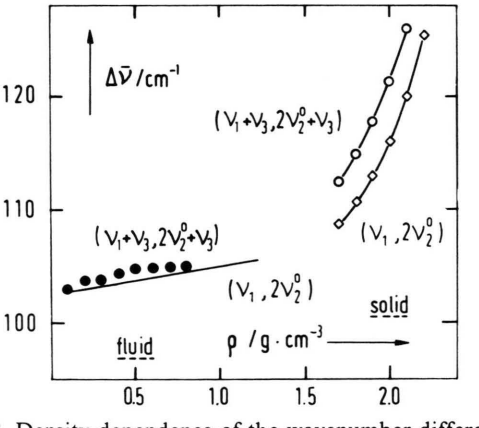

Fig. 3. Density dependence of the wavenumber difference, $\Delta\bar{\nu}$, between he maxima of Fermi diad components in pure CO_2. ● ($\nu_1+\nu_3$, $2\nu_2^0+\nu_3$) NIR fluid state data (298 K to 500 K), this work; — ($\nu_1, 2\nu_2^0$) Raman fluid state data (270 K to 315 K), Ref. [10]; ○ ($\nu_1+\nu_3$, $2\nu_2^0+\nu_3$) NIR solid state data (298 K), Ref. [17]; ◇ ($\nu_1, 2\nu_2^0$) Raman solid state data (298 K), Ref. [17].

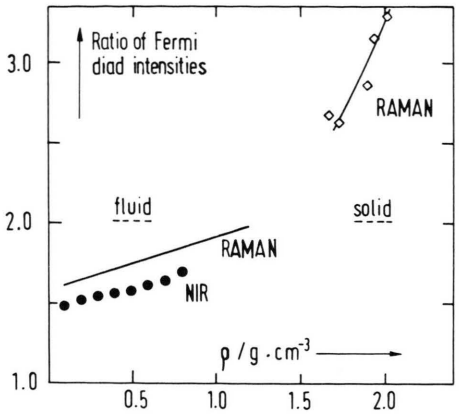

Fig. 4. Density dependence of the ratio of Fermi diad intensities (the higher wavenumber component is divided by the corresponding lower wavenumber component) in Raman scattering and NIR absorption spectra of pure CO_2. ● $(\nu_1 + \nu_3,\ 2\nu_2^0 + \nu_3)$ NIR fluid state data (298 K to 500 K), this work; —— $(\nu_1, 2\nu_2^0)$ Raman fluid state data (270 K to 315 K), Ref. [10]; ◇ $(\nu_1, 2\nu_2^0)$ Raman solid state ata (298 K), Ref. [17].

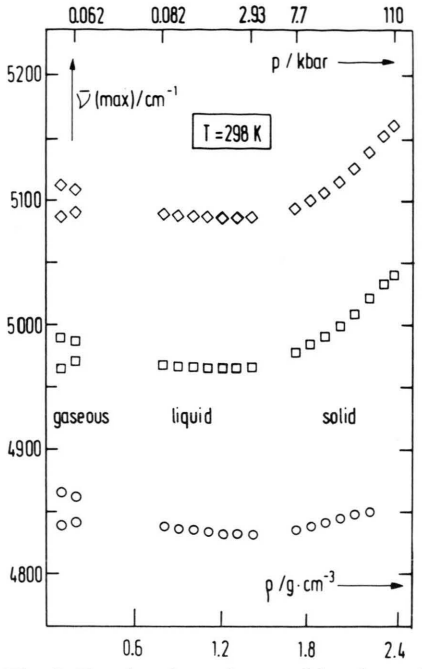

Fig. 5. Density dependence of band maximum positions, $\bar{\nu}(\max)$, of Fermi triad $2\nu_1 + \nu_3$, $\nu_1 + 2\nu_2^0 + \nu_3$, $4\nu_2^0 + \nu_3$ components in pure gaseous, liquid, and solid CO_2 at 298 K (solid state data are from Ref. [17]).

In the 5000 cm^{-1} region, where three modes $(2\nu_1 + \nu_3,\ \nu_1 + 2\nu_2 + \nu_3,\ 4\nu_2 + \nu_3)$ are coupled via Fermi resonance, the component analysis with determination of unperturbed frequencies is more complicated. Maximum wavenumbers $\bar{\nu}(\max)$ of the three bands observed at 298 K in gaseous, liquid, and solid CO_2 [17] are plotted versus density in Figure 5. Changes of $\bar{\nu}(\max)$ with density are weak for liquid as compared to solid states and, moreover, have opposite sign. The relatively weak blue-shift of the lowest wavenumber component on increasing solid density suggests an assignment of this species essentially to the $4\nu_2 + \nu_3$ mode with maximum bending type character. The two species at higher wavenumber (Fig. 5) have an almost identical density dependence. A firm conclusion about the size of unperturbed wavenumbers $(2\bar{\nu}_1 + \bar{\nu}_3)^u$ and $(\bar{\nu}_1 + 2\bar{\nu}_2 + \bar{\nu}_3)^u$ cannot be drawn, especially as solid state intensity data are not available.

The density and temperature dependence of the band maximum position, $\bar{\nu}(\max)$, of the most intense component of the Fermi triad with gaseous frequency $\bar{\nu}^g$ at 4977.8 cm^{-1}, is shown for an extended fluid range in Figure 6. At low density, P- and R-branches are observed. The R-branch maximum positions increase, and those of P-branches decrease with temperature, which demonstrates an appreciable rotational freedom in fluid CO_2 at moderate compression up to about the critical density (0.45 g · cm^{-3}). From about 0.6 g · cm^{-3} toward higher densities, bands with a single maximum occur (Figure 2). The peak position decreases along a straight line through $\bar{\nu}^g$ and through the mean values, $\bar{\nu}_m$, of the P- and R-branch maxima, as is shown in Figure 6. The maximum wavenumbers are independent of temperature, which indicates a severe restriction of free rotation. Above 0.9 g · cm^{-3} the $\bar{\nu}(\max)$ values deviate from the dashed straight line toward higher wavenumbers. They become independent of density and, at the highest fluid density, $\bar{\nu}(\max)$ seems to increase again. Thus the pronounced blue-shift with density which dominates the solid state CO_2 spectra (Fig. 5) is already weakly indicated in the very dense fluid state. Initial red-shifts of $\bar{\nu}(\max)$ on applying pressure with subsequent blue-shift behaviour toward the highest pressures have been reported for several materials by Drickamer's group [23, 24]. Following their interpretation, the high-density behaviour of $\bar{\nu}(\max)$ in CO_2 (Fig. 6) indicates that repulsive interactions strongly come into play at densities above 0.9 g · cm^{-3}.

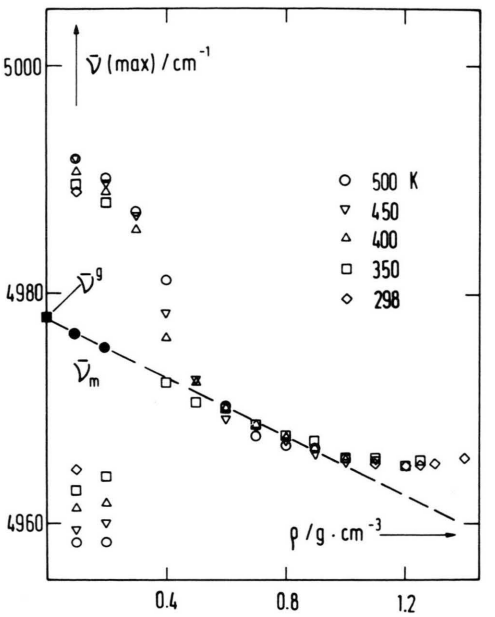

Fig. 6. Density dependence of band maximum position, $\bar{\nu}$(max), of the most intense Fermi triad component (with $\bar{\nu}^g$ at 4977.8 cm^{-1}) in pure CO_2 at temperatures between 298 K and 500 K ($\bar{\nu}_m$ is the arithmetic mean of corresponding P- and R-branch maxima).

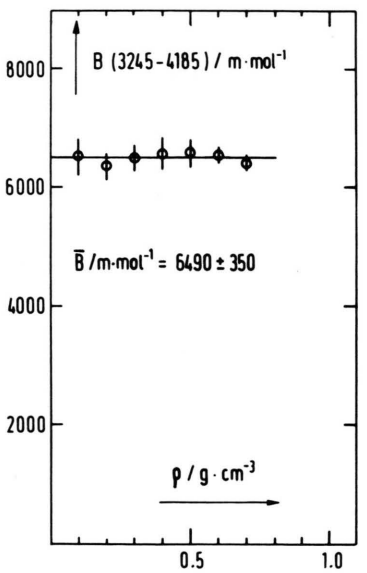

Fig. 7. Density dependence of the integrated molar absorptivity B of pure CO_2 in the wavenumber range from 3245 cm^{-1} to 4185 cm^{-1} (data points are mean values for the temperature range 298 K to 500 K).

A density and temperature dependence as in Fig. 6 is observed for most of the combination and overtone bands in pure CO_2 including the wavenumber region up to 7400 cm^{-1} [25]. Slight discrepancies are found in the extent to which $\bar{\nu}$(max) is blue-shifted at high fluid density. Moreover, deviations from the behaviour in Fig. 6 occur in that the density where the P- and R-branches coalesce into one temperature-independent band maximum can be shifted to values above 0.6 g · cm^{-3}, which may be due to rotational freedom around and perpendicular to the symmetry axis, this being different for vibrational modes with non-identical and, also because of Fermi coupling, density dependent stretching and bending contributions.

Because of the density dependent vibrational intensity transfer between Fermi coupled species as is illustrated in Fig. 4, absorbances of individual bands within Fermi diads or triads are no suitable measure of CO_2 concentration in wide ranges of pressure and temperature. Thus molar integrated absorptivities B are taken as a sum over resonating species. The $\nu_1 + \nu_3$, $2\nu_2 + \nu_3$ integration extends from 3245 cm^{-1} to 4185 cm^{-1}. B (3245–4185) as determined according to (1) is plotted versus density in Figure 7. The B's are arithmetic means of data measured between 298 K and 500 K. Within the limits of experimental accuracy, a density (and temperature) independent vibrational intensity of $B(3245-4185) = 6490 \pm 350$ m · mol^{-1} is found. Among the published gaseous $\nu_1 + \nu_3$, $2\nu_2 + \nu_3$ vibrational intensities [14, 26–28], Eggers and Crawford's value of 6580 m · mol^{-1} [26] is in almost perfect agreement. The other data deviate by up to 20%.

CO_2 fluid state vibrational intensities contain hot-band absorptions from the first excited level of ν_2 (at about 670 cm^{-1}) which may have transition matrix elements different from the corresponding ground state values. The temperature range of the present investigation is too small to precisely measure differences of this kind. There is a weak indication of the hot-band matrix elements being larger but the effect is too small to be clearly established. At very high temperature, above 1200 K, B has been found to increase with temperature [29]. The observation of $B(3245-4185)$ being independent of density (0.1 g · cm^{-3} to 0.7 g · cm^{-3}) and temperature (298 K to 500 K) indicates promis-

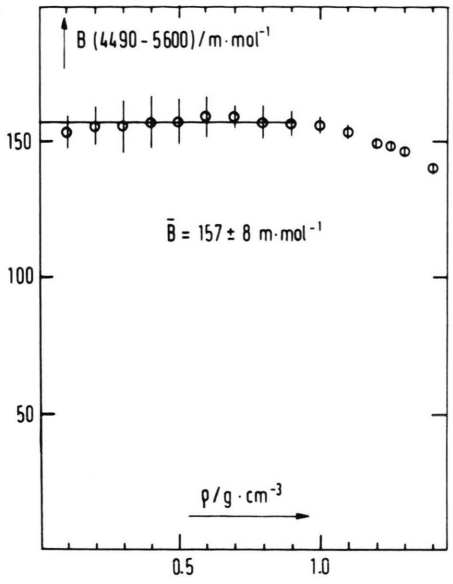

Fig. 8. Density dependence of the integrated molar absorptivity B of pure CO_2 in the wavenumber range from 4490 cm^{-1} to 5600 cm^{-1} (data points are mean values for the temperature range 298 K to 500 K).

ing applications of NIR spectroscopy in quantitative analysis of CO_2 in the fluid state.

Because of lower vibrational intensity, the Fermi triad $2\nu_1+\nu_3$, $\nu_1+2\nu_2+\nu_3$, $4\nu_2+\nu_3$ could be measured to higher densities. The integration is performed from 4490 cm^{-1} up to 5600 cm^{-1}. Mean values of $B(4490-5600)$ for temperatures between 298 K and 500 K are plotted versus density in Figure 8. The arithmetic mean of vibrational intensities between 0.1 $g \cdot cm^{-3}$ and 0.9 $g \cdot cm^{-3}$ is: $B(4490-5600) = 157 \pm 8$ $m \cdot mol^{-1}$. This value nicely agrees with recent gas phase literature data: 151.8 $m \cdot mol^{-1}$ (Schurin and Ellis [30]), 153.7 $m \cdot mol^{-1}$ (Downing and Hunt [14]), and 155.2 $m \cdot mol^{-1}$ (Rothman and Benedict [31]).

Above 0.9 $g \cdot cm^{-3}$, $B(4490-5600)$ decreases toward higher densities. The effect, which occurs well beyond the limits of experimental accuracy, indicates, as does the peak position of combination modes (Figs. 5 and 6), that repulsive interactions come into play. Changes of the molar integrated absorptivity B with density pose some problems for a precise spectroscopic determination of CO_2 concentration as the experimental absorbance $\int A(\bar{\nu}) \cdot d\bar{\nu}$ has a twofold dependence on concentration or density:

$$\int A(\bar{\nu})\, d\bar{\nu} = c\, l \int \varepsilon(\bar{\nu})\, d\bar{\nu} = c\, l\, B, \qquad (3)$$

and at well-known optical pathlength l, only the product $c\,B$ is directly obtained from the spectra. There is, however, an extended region of states up to about 1.0 $g \cdot cm^{-3}$ where the triad vibrational intensity is adequately represented by a single value of B, which is constant within $\pm$ 2.5%. This accuracy seems to be within reach in quantitative studies on fluid CO_2 to a maximum density of 1.0 $g \cdot cm^{-3}$ between 298 K and 500 K corresponding to pressures of 367 bar and 2200 bar, respectively. The triad absorption is especially interesting for analytical purposes as CO_2 concentrations may be determined in the presence of hydrocarbons and of carbon monoxide, which both have no absorption bands in the 5000 cm^{-1} region. Even in mixtures with materials where appreciable band overlap occurs, knowledge of the pure component spectra, via routine computer programs, may enable the spectrum of the mixture to be resolved into NIR component spectra and thus to derive the concentration of species.

Within the present paper, the analysis of the density and temperature dependence of band positions and of vibrational intensities suffered from problems due to Fermi coupling and partly also to hot-band transitions. The second overtone of the anharmonic stretching fundamental, $3\nu_3$, with gaseous frequency $3\bar{\nu}_3^g$ at 6972.6 cm^{-1}, does not participate in any Fermi resonance interaction and, at low temperature, has only a small or even negligible hot-band contribution [18]. The NIR absorption of $3\nu_3$, up to high pressures and temperatures, is studied in Part II of this paper, which refers to the wavenumber range 5600 cm^{-1} to 7400 cm^{-1} where, in addition to the uncoupled $3\nu_3$ mode, the Fermi tetrad $3\nu_1+\nu_3$, $2\nu_1+2\nu_2+\nu_3$, $\nu_1+4\nu_2+\nu_3$, $6\nu_2+\nu_3$ occurs around 6300 cm^{-1}.

Acknowledgements

Financial support by the Deutsche Forschungsgemeinschaft (SFB 93) and by the Fonds der Chemischen Industrie is gratefully acknowledged. One of us, H.T., would like to thank the Max-Buchner-Forschungsstiftung for a fellowship.

[1] E. U. Franck and K. Roth, Discuss. Faraday Soc. **43,** 108 (1967).
[2] M. Buback and E. U. Franck, J. Chim. Phys. **72,** 601 (1975).
[3] M. Buback and F. W. Nees, Ber. Bunsenges. Phys. Chem. **80,** 650 (1976).
[4] M. Buback, J. Schweer, and H. Tups, Ber. Bunsenges. Phys. Chem. **89,** 545 (1985).
[5] M. Buback, Z. Naturforsch. **39a,** 399 (1984).
[6] E. U. Franck, Ber. Bunsenges. Phys. Chem. **88,** 820 (1984).
[7] G. M. Schneider, Ber. Bunsenges. Phys. Chem. **88,** 841 (1984).
[8] G. Herzberg, Infrared and Raman Spectra of Polyatomic Molecules, Van Nostrand, Princeton, New York 1945.
[9] C. P. Courtoy, Can. J. Phys. **35,** 608 (1957) and Ann. Soc. Sci. Bruxelles **73,** 5 (1959).
[10] Y. Garrabos, R. Tufeu, B. Le Neindre, G. Zalczer, and D. Beysens, J. Chem. Phys. **72,** 4637 (1980).
[11] J. F. Bertran, Spectrochim. Acta **39A,** 119 (1983) and references therein.
[12] W. C. Waggener, A. J. Weinberger, and R. W. Stoughton, J. Phys. Chem. **71,** 4320 (1967).
[13] H. D. Downing and R. H. Hunt, J. Quant. Spectrosc. Radiat. Transfer **13,** 311 (1973).
[14] H. D. Downing, L. R. Brown, and R. H. Hunt, J. Quant. Spectrosc. Radiat. Transfer **15,** 205 (1975).
[15] J.-Y. Mandin, J. Mol. Spectrosc. **67,** 304 (1977).
[16] F. P. J. Valero, C. B. Suárez, and R. W. Boese, J. Quant. Spectrosc. Radiat. Transfer **22,** 93 (1979); **23,** 337 (1980).
[17] R. C. Hanson and L. H. Jones, J. Chem. Phys. **75,** 1102 (1981).
[18] L. S. Rothman and L. D. G. Young, J. Quant. Spectrosc. Radiat. Transfer **25,** 505 (1981).
[19] Ph. Arcas, E. Arié, M. Cuisenier, and J. P. Maillard, Can. J. Phys. **61,** 857 (1983).
[20] M. Buback and H. Lendle, Z. Naturforsch. **34a,** 1482 (1979); M. Buback and A. A. Harfoush, Z. Naturforsch. **38a,** 528 (1983).
[21] A. Michels, C. Michels, and H. Wouters, Proc. Roy. Soc. London **A 153,** 214 (1935).
[22] IUPAC International Thermodynamic Tables of the Fluid State, CO_2, Butterworths, London 1973.
[23] A. M. Benson and H. G. Drickamer, J. Chem. Phys. **27,** 1164 (1957).
[24] R. R. Wiederkehr and H. G. Drickamer, J. Chem. Phys. **28,** 311 (1958).
[25] M. Buback, J. Schweer, and H. Tups, Z. Naturforsch. **41a,** 512 (1986).
[26] D. F. Eggers and B. L. Crawford, J. Chem. Phys. **19,** 1556 (1951).
[27] D. Weber, R. G. Holm, and S. S. Penner, J. Chem. Phys. **20,** 1820 (1952).
[28] D. E. Burch, D. A. Gryvnak, R. A. Patty, and C. E. Bartky, J. Opt. Soc. Amer. **59,** 267 (1969).
[29] J. C. Breeze and C. C. Ferriso, J. Chem. Phys. **39,** 2619 (1963); **40,** 1276 (1964).
[30] B. D. Schurin and R. E. Ellis, Appl. Opt. **7,** 467 (1968).
[31] L. S. Rothman and W. S. Benedict, Appl. Opt. **17,** 2605 (1978).